Creation of "Quantum Platelets" via Strain-Controlled Self-Organization at Steps

Adam Li, Feng Liu,* D. Y. Petrovykh, J.-L. Lin, J. Viernow, F. J. Himpsel, and M. G. Lagally
University of Wisconsin, Madison, Wisconsin 53706
(Received 23 August 2000)

We demonstrate, by both theory and experiment, the strain-induced self-organized formation of "quantum platelets," monolayer-thick islands of finite dimensions. They form at the early stage of heteroepitaxial growth on a substrate with regularly spaced steps, and align along the steps. In the direction perpendicular to substrate steps, the island position and spacing can be preselected through substrate miscut. Along the steps, the island size and density are controlled by self-organized growth.

PACS numbers: 81.15.Kk, 68.35.Md

Nature exhibits a wealth of fascinating self-assembly and self-organization processes. They lead to beautiful patterns in a wide range of length scales, from cosmic arrays of galaxies to the atomic structure of crystals. Recently there has been intense interest in employing self-organization processes to synthesize exotic materials, in particular, those whose structural patterns lie in the nanometer scale, as they form the building blocks for potentially novel electronic and optoelectronic devices. There are a number of such processes [1–8]; we focus here on heteroepitaxial growth (material B on A) of thin films, in which lattice misfit strain induces self-organization of three-dimensional (3D) islands [4–6], step bunches [7], and alloy superlattices [8].

If self-organization processes operating at different length scales can be combined, it may be possible to obtain unique patterns or better control of the patterns that form. For example, heteroepitaxial growth can be carried out on a vicinal substrate, created by miscutting the sample a few degrees away from a low-Miller-index surface. A vicinal substrate often consists of a self-organized staircase of equally spaced steps that defines one length scale. The self-organization of the deposited material can occur on a finer scale, superimposed on the staircase.

On a vicinal substrate, one may expect approximate 2D analogs of all the 3D equilibrium growth modes [9] [Frank–van der Merwe (FV), Stranski-Krastanov (SK), and Volmer-Weber (VW)], as illustrated in Fig. 1. They are determined by the balance between interstep energy (laterally between the film and the substrate steps, equivalent to interfacial energy in 3D) and energies of film steps and substrate steps (equivalent to surface energies in 3D). For homooepitaxy on a vicinal substrate with terrace width W [Fig. 1(b)], one would expect "ideal step flow growth," i.e., stripes of the deposited material with width $w = \theta W$ at every step at a film coverage θ. For heteroepitaxy, i.e., if misfit strain is present, we expect, depending on the magnitude of the misfit strain, the formation of a stress domain structure, either with [Fig. 1(d), SK growth] or without [Fig. 1(f), VW growth] a "wetting stripe" (corresponding to the wetting layer in 3D case).

Stranski-Krastanov growth has already been widely used for strain-induced self-organized formation of 3D nanostructures [10]. One may then ask whether a similar approach for nanofabrication can be applied in the growth of strained 2D layers. In this Letter, we demonstrate such a possibility, by both theory and experiment. We show that strain caused by lattice mismatch between the deposited material and the substrate induces a generic instability against step flow at the initial stage of heteroepitaxy, leading to the formation of arrays of 2D (monolayer thick) islands along the substrate steps, which look like small plates. We therefore coin the name "quantum platelets" to describe them. Furthermore, strain induces a long-range elastic interaction between islands on different terraces,

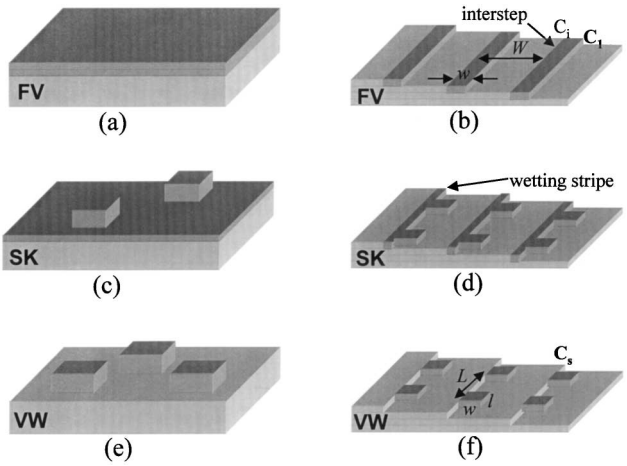

FIG. 1. 2D analogs of 3D equilibrium growth mode, occurring during step flow growth on a vicinal substrate. (a) 3D Frank–van der Merwe (FV) mode, layer-by-layer growth. (b) 2D FV mode, row-by-row growth. Continuous stripes formed under "ideal" step flow. W is the terrace width of underlying substrate; w is the width of the growing stripes. (c) 3D Stranski-Krastanov (SK) mode, layer-by-layer followed by island growth. (d) 2D SK mode, row-by-row followed by island growth. (e) 3D Volmer-Weber (VW) mode, island growth. (e) 2D VM mode, island growth. To facilitate the energy calculation, the islands are assumed to be rectangular in shape and periodically arrayed. Each island has a size of length $l = \alpha L$ and width $w = \beta W$. L is the periodicity in the direction along the substrate step.

 0031-9007/00/85(25)/5380(4)$15.00

as they form simultaneously along all the steps (multiple growth fronts, in contrast to only one growth front in the 3D case). This interaction plays an important role in defining the evolution of island morphology. In the direction perpendicular to steps, the quantum platelets have a perfect positional order defined by substrate miscut; along the substrate steps, the platelet size and density is controlled by the self-organized growth process.

Consider the heteroepitaxial growth of a layer on a vicinal substrate with terrace width W [Figs. 1(b), 1(d), and 1(f)]. If the growth proceeded by "ideal" step flow, stripes of the deposited material with width $w = \theta W$ would form at every step at a film coverage θ [Fig. 1(b)]. Misfit strain induces a force monopole on both edges of the stripes with a magnitude proportional to the misfit strain and the step height [7], forming in effect a stress domain structure [11]. [One edge of the stripe is a free step edge, the other is buried, forming an "interstep" with the buried substrate step edge; see Fig. 1(b).] The total energy per unit area, E_{stripe} can be written as

$$E_{\text{stripe}} = \frac{1}{W}\left[C_i + C_1 - 2C_2 \ln\left(\frac{W}{2\pi a}\sin\pi\theta\right)\right], \quad (1)$$

where C_i is the "interstep" energy per unit length, i.e., the vertical interface between the "buried" (in a lateral sense) stripe edge and the buried substrate step, C_1 is the step energy per unit length of the free edge of the stripe, and C_2 is a constant related to the force monopole and the elastic constants of the substrate. a is a cutoff length of the order of the surface lattice constant.

The strain contribution to E_{stripe} [the last term in Eq. (1)] depends on the coverage θ, as shown in Fig. 2 (solid line). It is very high at very low coverage because of the strong *intrastripe* repulsion between the monopoles on the opposite edges of the same stripe. It decreases with increasing film coverage and reaches a minimum at half-monolayer coverage ($\theta = 1/2$). At higher coverages, the energy increases and becomes very high again as the coverage approaches one monolayer, because of the strong *interstripe* repulsion between monopoles on opposing edges of two neighboring stripes.

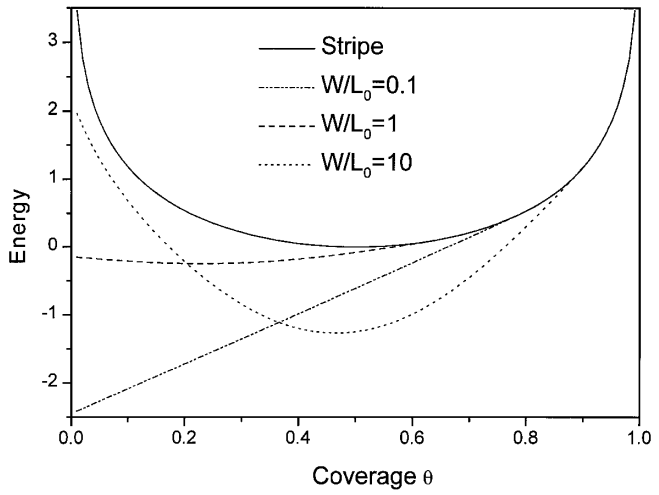

FIG. 2. The strain energy per unit area of the stripe configuration (the solid line) and of the island configuration (the broken lines) for different values of W/L_0, i.e., the ratio of the substrate terrace width (W) and the size of stable isolated island (L_0). The island configuration always has lower strain energy than the stripe configuration at the beginning of the growth (low coverage) for any W/L_0.

The initial divergence of strain energy can be greatly relaxed by roughening of the lateral growth fronts, which may occur in different forms. To illustrate the instability, we consider a particular form of relaxation, corresponding to the 2D analog of the Volmer-Weber mode, in which the stripe breaks up into arrays of 2D islands attached to the substrate steps, with no "wetting stripes" between the islands [Fig. 1(f)].

We assume islands form a 2D periodic array with a periodicity L along the substrate step direction (in the orthogonal direction, the periodicity is fixed by the terrace width W), with a length $l = \alpha L$ and width $w = \beta W$ [Fig. 1(f)]. It is easy to see that $\alpha\beta = \theta$, $\theta \le \alpha \le 1$, and $\theta \le \beta \le 1$. Thus, at a given coverage, the island configuration is defined by two independent variables, L and α (or β). It can be shown that the optimal island configuration (i.e., optimal values of L and α) must satisfy the following equation:

$$\beta\left[\pi\cot\pi\beta + \frac{W}{L_0}\left(\frac{2}{\alpha}\sin\pi\alpha - \cos\pi\alpha\right)\right] + \ln\frac{L_0\pi}{We\sin\pi\beta} + \frac{C_i - C_s - C_1}{2C_2} = 0, \quad (2)$$

where $L_0 = 2ae^{(C_1/C_2)+1}$ is the stable size of an isolated island [12] and C_s is the substrate step energy. The total energy per unit area of the corresponding island array is

$$E_{\text{island}} = \frac{2C_2}{W}\left[-\beta\frac{W\sin\pi\alpha}{L_0\pi} + \alpha\ln\frac{L_0\pi}{We\sin\pi\beta} + \frac{\alpha}{2C_2}(C_i - C_s - C_1) + \frac{1}{2C_2}C_s\right]. \quad (3)$$

As expected, E_{island} in Eq. (3) reduces to E_{stripe} in Eq. (1) for $\alpha = 1$ and $\beta = \theta$.

For systems in which strain energy dominates step energies (i.e., $C_2 \gg |C_i - C_s - C_1|$), the island morphology is solely defined by a single parameter, W/L_0, the ratio of the substrate terrace width, and the stable size of an isolated island. The strain energy of the optimal island array [neglecting the last two terms in Eq. (2)] is plotted in Fig. 2 as a function of coverage for different values of W/L_0, in comparison to that of the continuous stripes. The islands have a lower energy than stripes at low coverages, independent of the choice of W/L_0, indicating a generic breakdown of initial step flow.

The evolution of equilibrium island morphology with increasing coverage is determined by energy minimization of stress domains [12]. It varies with W/L_0, under the specific boundary conditions of constrained island locations and shapes along the substrate steps. If the terrace

size is much larger than the stable size of a single island, i.e., $W \gg L_0$, the interaction between islands on different terraces is initially negligible. Thus, at very low coverage, when $\theta \ll 1$, $\alpha \ll 1$, and $\beta \ll 1$, we have $L = L_0^2/W\theta$ and $\alpha L = \beta W = L_0$, indicating that all islands initially form with a size of $L_0 \times L_0$, as isolated stable platelets; and the platelet separation along the substrate steps is defined by the coverage, with $L = L_0^2/W\theta$, which decreases with increasing coverage. As the coverage increases to a point where the separation approaches the optimal value $\sim L_0$, platelets begin to grow *perpendicular* to the substrate steps, in an attempt to form optimally spaced stripes perpendicular to the steps. As the coverage increases further, the repulsion between platelets on *neighboring* terraces becomes significant, and platelets stop growing perpendicular to the steps. They begin to grow along the steps, and gradually merge into continuous stripes, eventually converting to step flow growth.

If the terrace size is comparable to the stable size of a single island, the repulsion between islands on different terraces (i.e., in the β direction) is strong from the very beginning. Consequently, islands initially adopt an optimal length of L_0 along the steps and a width of $\sim W/2$ perpendicular to the steps. As the coverage increases, they first increase their density (reducing their separation) and then grow predominantly along the steps until coalescence, after which growth continues via step flow.

The spontaneous island formation we show here provides a pathway for growing 2D quantum dots, or quantum "platelets." It represents a natural combination of strain-induced self-organization and a patterned substrate. The islands are confined to form along the substrate steps, so we achieve a nearly perfect control of spacing in the direction perpendicular to the substrate steps. The island morphology, i.e., island size and density (spacing along the substrate steps), can also be controlled by tuning the parameter W/L_0, where W can be adjusted by changing the substrate miscut angle and L_0 can be adjusted by changing the film composition when this is feasible.

We provide an experimental example supporting this picture. We have reproducibly obtained large areas of high-quality stepped surfaces on vicinal Si(111) using a special preparation procedure described elsewhere [13]. As an example of a strained heteroepitaxial system, CaF_2 was deposited on such vicinal Si(111) substrates. The lattice mismatch is 0.6% at room temperature and 2.4% at typical growth temperatures of $600 \sim 650\,^{\circ}\mathrm{C}$ [14]. Si(111) samples miscut 1° towards $(\bar{1}\,\bar{1}2)$ direction were used as substrates. CaF_2 was deposited from a resistively heated BN cell at a growth rate of approximately 1 monolayer (ML) per minute.

At low coverages, the growth results in strings of islands attached to step edges (Fig. 3 top), i.e., something resembling a 2D VW mode. The islands remain at nearly constant width of half of the substrate terrace width, as they grow along the substrate steps and merge into continuous stripes. This experiment corresponds directly to the theory. The constant island width of half of the substrate terrace width before islands merge indicates the system is likely in the regime of $L_0 \sim W$.

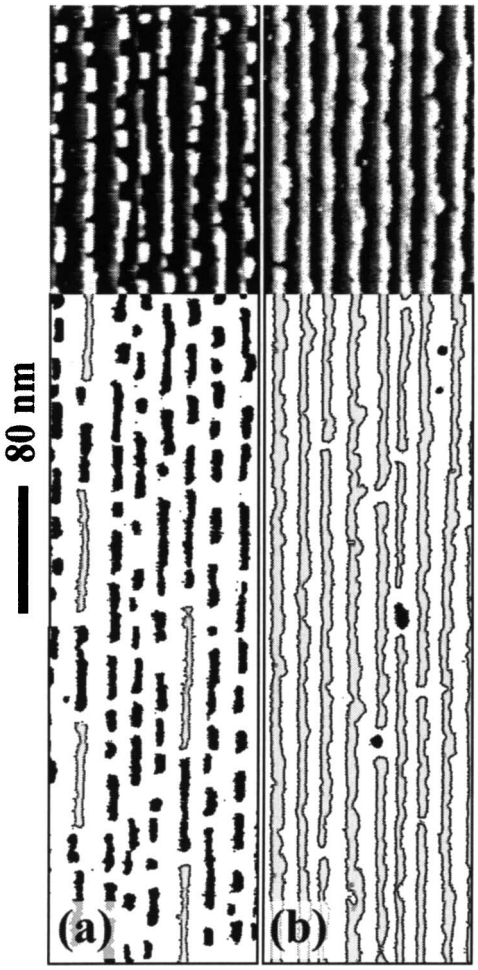

FIG. 3. STM images of CaF_2 on stepped Si(111), showing the transition from platelets to stripes. The two samples are prepared under the same conditions, except for the coverage, 0.23 ML in (a) and 0.40 ML in (b). Top portion of the images shows STM topography, bottom is color coded—platelets [black, dominant in (a)] and stripes [gray, longer than 80 nm, dominant in (b)].

At high coverages, the step flow growth mode is observed for the growth conditions described above [15]. These continuous stripes are obtained only for coverages above $\sim$0.4 ML. This feature also arises in the calculation. The equilibrium island configuration is determined by minimizing the repulsive interaction between islands. At a given growth stage, which side of the islands grows preferentially depends on the direction (α or β) in which the island-island repulsion is dominant. Eventually, the interaction between islands on different terraces can effectively suppress the roughening and always drives the islands, beyond a critical coverage below one monolayer, to merge into continuous stripes along the substrate steps. Such a morphological transition from initially rough to smooth represents a kind of inverse SK growth mode. The critical coverage (i.e., the stripe width) for the transition can be determined by the condition that the minimum of

E_{island} is at the configuration $\alpha = 1$ and $\beta = \theta$. From Eq. (2), we have

$$\theta_c\left(\pi \cot \pi\theta_c + \frac{W}{L_0}\right) + \ln \frac{L_0 \pi}{We \sin \pi\theta_c} + \frac{C_i - C_s - C_1}{2C_2} = 0. \quad (4)$$

The first two terms on the left-hand side of Eq. (4) make a monotonically decreasing function of θ_c between 0 and 1; the last term is negative for islands attaching to the substrate step edges [16]. Consequently, solving the equation with the last term neglected (i.e., neglecting the step energy contribution) will give the upper limit for the critical coverage θ_c (see Fig. 4), which is solely determined by W/L_0. The effect of step energy (in particular, a large C_i) will lower the critical coverage.

The rough-to-smooth morphological transition beyond a critical coverage observed in the experiment is in good agreement with the unusual inverse SK growth mode predicted by our theory. The measured critical coverage ($\sim$0.4 ML) is below the predicted *minimum* upper limit ($\sim$0.6 ML), indicating a large interstep energy between CaF_2 and Si(111). The experimentally measured critical coverage is increased to ($\sim$0.5 ML) when the substrate terrace width is decreased by a factor of $\sim$2 by doubling the substrate miscut angle. This further indicates that the system falls into the regime of $W < L_0$ (i.e., on the left side of the minimum in Fig. 4).

The critical smoothening phenomenon may be used for growing quantum wires with a control of minimum wire width. In particular, the smoothening mechanism tends to make the wires smoother.

In conclusion, we have demonstrated a strain induced instability at the early stage (submonolayer coverage) of heteroepitaxial growth on vicinal substrates. The growth fronts are initially rough, forming 2D platelike islands to reduce strain energy. As the growth proceeds, the strain induced interaction between the islands formed on different terraces eventually smoothens the growth front whereupon step flow growth begins. This latter morphological transition, from rough to smooth, is a novel aspect of growth with multiple laterally interacting growth fronts. The upper limit of the critical coverage is solely determined by the ratio of the substrate terrace width and the stable size of an isolated island under strain. We expect that this growth mode, in its initial form, may be useful for fabricating arrays of quantum platelets with potentially novel electronic properties. At the later stage, the critical smoothening phenomenon may be used for growing quantum wires with a control of minimum wire width. In particular, the smoothening mechanism tends to make the wires smoother.

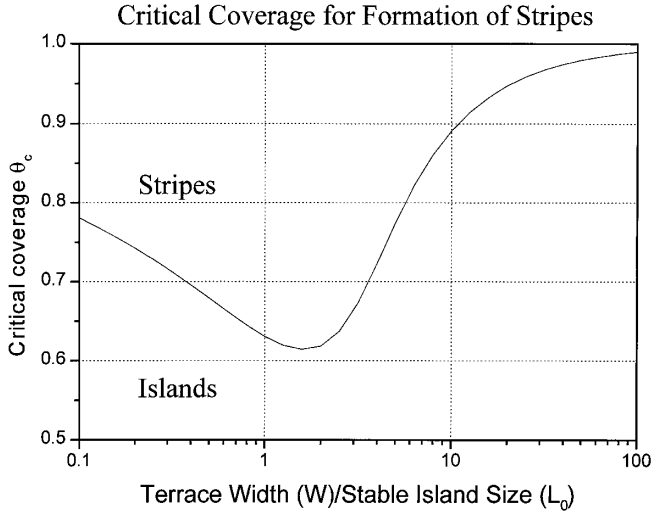

FIG. 4. The upper limit of critical coverage θ_c, for transition from rough growth fronts (platelets) to smooth growth fronts (stripes), as a function of the ratio of the width of substrate terrace and the stable size of a single island (W/L_0).

This work was supported by NSF, Grants No. DMR-9632527, No. DMR-9304912, No. DMR-9632527, and No. DMR-9815416, and by DOE, Grant No. DE-FG02-00ER45816.

*Present address: University of Utah, Salt Lake City, UT 84112.

[1] E. L. Thomas, Science **286**, 1307 (1999).
[2] N. Bowden, S. Brittain, and G. M. Whitesides, Nature (London) **393**, 146 (1998).
[3] C. B. Murray, C. R. Kagan, and M. G. Bawendi, Science **270**, 1335 (1995).
[4] V. A. Shchukin, N. N. Ledentsov, P. S. Kop'ev, and D. Bimberg, Phys. Rev. Lett. **75**, 2968 (1995).
[5] J. Tersoff, C. Teichert, and M. G. Lagally, Phys. Rev. Lett. **76**, 1675 (1996).
[6] Feng Liu, S. E. Davenport, H. M. Evans, and M. G. Lagally, Phys. Rev. Lett. **82**, 2528 (1998).
[7] Feng Liu, J. Tersoff, and M. G. Lagally, Phys. Rev. Lett. **80**, 1268 (1998).
[8] P. Venezuela, J. Tersoff, J. A. Floro, E. Chason, D. M. Follstaedt, Feng Liu, and M. G. Lagally, Nature (London) **397**, 678 (1998).
[9] E. Ball, Z. Kristallogr. **110**, 372 (1958).
[10] Feng Liu and M. G. Lagally, Surf. Sci. **386**, 169 (1997).
[11] V. I. Marchenko and A. Y. Parshin, Sov. Phys. JETP **52**, 129 (1980); O. L. Alerland, D. Vanderbilt, R. D. Meade, and J. D. Joannopoulos, Phys. Rev. Lett. **61**, 1973 (1988).
[12] K. O. Ng and D. Vanderbilt, Phys. Rev. B **52**, 2177 (1995).
[13] J. Viernow, J.-L. Lin, D. Y. Petrovykh, F. M. Leibsle, F. K. Men, and F. J. Himpsel, Appl. Phys. Lett. **72**, 948 (1998); J.-L. Lin, D. Y. Petrovykh, J. Viernow, F. K. Men, D. J. Seo, and F. J. Himpsel, J. Appl. Phys. **84**, 255 (1998).
[14] M. A. Olmstead, in *Heteroepitaxial Systems,* edited by Amy W. K. Liu and Michael Santos (World Scientific, Singapore, 1998), Chap. 5.
[15] J. Viernow, D. Y. Petrovykh, F. K. Men, A. Kirakosian, J.-L. Lin, and F. J. Himpsel, Appl. Phys. Lett. **74**, 2125 (1999).
[16] Adam H. Li, Feng Liu, and M. G. Lagally (to be published).